Dentomaxillofacial Radiology (2022) 51, 20210092

birpublications.org/dmfr

RESEARCH ARTICLE

CBCT image artefacts generated by implants located inside the field of view or in the exomass

[1]Husniye Demirturk Kocasarac, [1]Lisa J Koenig, [2]Gulbahar Ustaoglu, [3]Matheus Lima Oliveira and [3]Deborah Queiroz Freitas

[1]Division of Oral and Maxillofacial Radiology, Department of General Dental Sciences, Marquette University School of Dentistry, Milwaukee, Wisconsin, United States; [2]Department of Periodontics, Bolu Abant Izzet Baysal University Faculty of Dentistry, BAIBU Golkoy Yerleskesi, Merkez/Bolu, Turkey; [3]Division of Oral Radiology, Department of Oral Diagnosis, Piracicaba Dental School, University of Campinas, Piracicaba, Brazil

Objectives: To compare artefacts in cone-beam computed tomography (CBCT) arising from implants of different materials located either inside the field of view (FOV) or in the exomass, and to test different image-acquisition parameters to reduce them.
Methods: CBCT scans of a human mandible prepared with either a titanium, titanium–zirconium, or zirconia implant were acquired with the Planmeca ProMax utilizing FOV sizes of 8 × 5 cm and 4 × 5 cm, which placed the implant inside the FOV (8 × 5 cm) or in the exomass (4 × 5 cm). The scanning parameters considered three conditions of metal artefact reduction (MAR), disabled, low, and high, and 2 kVp levels (80 and 90). The standard deviation (SD) of grey values of regions of interest was obtained. The effects of implant material, implant position, MAR condition, kVp level, and their interactions were evaluated by Analysis of Variance ($\alpha = 5\%$).
Results: The zirconia implant produced the highest SD values (more heterogeneous grey values, corresponding to greater artefact expression), followed by titanium–zirconium, and titanium. In general, implants in the exomass produced images with higher SD values than implants inside the FOV. MAR was effective in decreasing SD values, especially from the zirconia implant, only when the implant was inside the FOV. Images with 80 kVp had higher SD values than those with 90 kVp, regardless of the other factors ($p < 0.05$).
Conclusions: Implants in the exomass lead to greater artefact expression than when they are inside the FOV. Special attention should be paid to scanning parameters that reduce metal-related artefacts, such as MAR activation and increasing kVp. This is especially important with a zirconia implant inside the FOV.
Dentomaxillofacial Radiology (2022) **51**, 20210092. doi: 10.1259/dmfr.20210092

Cite this article as: Demirturk Kocasarac H, Koenig LJ, Ustaoglu G, Oliveira ML, Freitas DQ. CBCT image artefacts generated by implants located inside the field of view or in the exomass. *Dentomaxillofac Radiol* 2022; **51**: 20210092.

Keywords: Zirconia; Titanium; X-Rays; CBCT; Artefacts

Introduction

Cone-beam computed tomography (CBCT) is a well-accepted diagnostic imaging modality for dental implant treatment planning, as well as for surgical, orthodontic, periodontal, and endodontic treatments. A well-known limitation of this modality is the occurrence of artefact, which is any entity visualised in the reconstructed image that does not represent real features of the assessed object. Artefacts result from discrepancies between physical characteristics of the object and the three-dimensional reconstruction algorithm.[1,2] Furthermore, the object and positioning in the field of view

Correspondence to: Dr Husniye Demirturk Kocasarac, E-mail: husniyedemirturk@gmail.com

Received 02 March 2021; revised 23 June 2021; accepted 17 July 2021

(FOV) might significantly interfere in the expression of artefact.[1,3]

During a CBCT scan, high-density objects, such as metal implants, absorb low-energy X-ray photons, which indirectly increase the average energy of the X-ray beam reaching the detector. This induces an error in data reconstruction, introducing dark bands and white streaks to the image, which may impair the image quality, increase the interpretation time, and reduce the diagnostic accuracy by masking structures of interest.[1–4]

Owing to inherent computational, energy-related, and geometric components of CBCT, voxel values are not accurate.[5–7] The CBCT voxel value variability forms artefacts in the reconstructed image,[1,5] decreasing diagnostic accuracy.[5,8,9] Modifying the CBCT exposure parameters to produce high-energy X-rays is an option to reduce the artefacts. Thus, kilovoltage (kVp) seems to be one of the foremost energy parameters that affects artefact generation.[2,4,10] Higher kVp generates higher mean energy photons which will be less absorbed by high-density objects. Importantly, higher kVp generally increases the radiation dose,[2,11] hence, high kVp should be restricted to situations when high image quality is needed to improve diagnostic accuracy.[2,12] Another effective way to reduce CBCT artefact is the use of metal artefact reduction (MAR) algorithms which are offered in some CBCT units. Because MAR algorithms are involved during image reconstruction, they do not affect radiation dose and image acquisition process.[2,13] Although CBCT manufacturers do not elucidate its mechanism, previous studies have suggested a threshold based on the mean grey values of the image is applied and any region more or less dense than the threshold is adjusted. So, grey value variation, hence artefact production, will be reduced.[2,14,15]

Currently, the use of small-FOV sizes has been increased due to the demand for high spatial resolution and reduced radiation dose.[5,16,17] However, a small FOV leads to an indirect increase of the exomass, described as the area between the source of X-rays and the image detector but outside of the FOV. Normally, CBCT reconstruction algorithms attempt to ignore the data from the exomass to avoid negative interference in the reconstructed images which is referred to as truncation correction.[5,18] Yet, metal objects in the exomass have been shown to generate inevitable artefacts due to inconsistent image reconstructions.[5,18,19]

The frequent use of small-FOV sizes and the significant number of patients having high-density materials in the oral cavity, not always within the FOV, presents an image acquisition challenge. For this reason, the goal of the present study was to compare the artefacts arising from implants of different materials located inside the FOV and in the exomass on CBCT images and to test different image-acquisition parameters which may reduce them.

Methods and materials

Phantom preparation

A dry human mandible was used to individually insert dental implants of three different materials: a 4.1 × 12 mm titanium–zirconium implant (Roxolid, Straumann, Basel, Switzerland), a 4 × 11 mm titanium implant (Titamax, Neodent, Curitiba, PR, Brazil), and a 4 × 11 mm zirconia implant (Z-Look3, Z-systems, Oensingen, Switzerland). Each implant was placed in the right posterior region of the mandible corresponding to the alveolar socket of the first molar, and a 9 × 4 × 4 mm epoxy resin-based (ERB) tissue substitute block was placed in the lingual cortical plate of the anterior region of the mandible, aligned to the middle line, to serve as a reference for further selection of the same axial view for analysis. The mid-height level of the ERB block coincided with the mid-height level of the implant. The mandible was fixed with impression material to the bottom of a polypropylene container (150 mm in diameter), which was filled with water to simulate X-ray interaction and attenuation with soft tissues.

CBCT scanning

The phantom with a titanium–zirconium, titanium or zirconia implant was individually scanned using the Planmeca ProMax 3D CBCT unit (Planmeca Oy, Helsinki, Finland) with the following fixed acquisition parameters: 5 mA, 0.15 mm voxel size, an exposure time of 12 s and a total of 251 frames. The following parameters were variable: kVp (80 or 90 kVp), MAR activation (without, low-level or high-level), and FOV size (8 × 5 cm or 4 × 5 cm). The position of the phantom was standardised by fixing it to the platform of the CBCT unit and following the laser lights of each FOV size. For the 8 × 5 cm FOV, the mandible was centred in the FOV, whereas for the 4 × 5 cm FOV, the left posterior region of the mandible was included in the FOV such that the implant was in the exomass, near the border of the FOV. Therefore, two positions of each implant were tested: the implant inside the FOV when an 8 × 5 cm FOV was used, and the implant in the exomass when a 4 × 5 cm FOV was used. Additionally, CBCT exams without an implant were acquired under the same parameters to serve as control scans. Each experimental condition was obtained in triplicate, totalling 144 CBCT scans [3 × (1 control + 3 implants) x 2 implant positions x 3 MAR conditions x 2 kVp levels]. Representative axial images according to parameters studied are in Figures 1 and 2.

Image analysis

A previously calibrated oral and maxillofacial radiologist with 10 years of experience assessed the CBCT scans under dim light conditions. For each CBCT scan, an axial reconstruction was determined in the mid-height level of the ERB block, which corresponded to the mid-height level of the implant. Using the ImageJ software (NIH Image, Bethesda, MD) and 16-bit images, 3

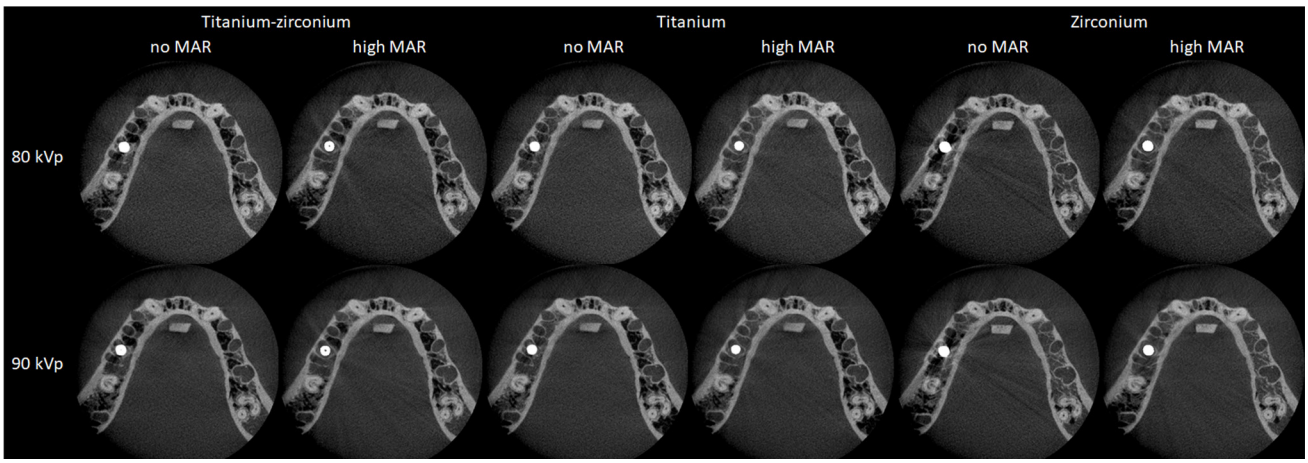

Figure 1 Representative CBCT axial images obtained with a 8 × 5 cm FOV according to the implant material, MAR condition, and kVp level. CBCT, cone-beam CT; FOV, field of view; MAR, metal artefact reduction.

rectangular regions of interest (ROIs) of 3.6 × 12 mm were placed on the axial images at three distances from the implant taking into account the ERB block and anatomic landmarks since the implant was not visualised in images with 4 × 5 cm FOV nor in control scans. One of the ROIs (middle ROI) was placed over the right-angle intersection between an imaginary horizontal line tangent to the mesial aspect of the alveolar socket of the left second premolar and a vertical line tangent to the ERBS block. The other two ROIs were horizontally aligned with the middle ROI, such that one ROI was 3.6 mm towards the implant and the other ROI was 3.6 mm in the opposite direction to the implant. (Figure 3). To ensure accurate reproducibility of the location of the ROIs in the axial images of CBCT scans obtained with the same FOV size, the Macro tool was used. This tool is a functionality of the ImageJ software that automates a series of internal commands. In the present study, the Macro tool recorded and reproduced the total number of pixels of each ROI with their corresponding x and y co-ordinates.

The standard deviation (SD) of the grey values was collected from all ROIs and used to objectively determine the expression of artefact.[13,14] Higher SD of the grey values represents greater voxel value variability, corresponding to greater artefact expression.

Statistical analysis

The SD of the grey values from the three ROIs of the same axial image were averaged and compared using multiway analysis of variance (ANOVA) with post-hoc Tukey test. These analyses evaluated the influence of each studied factor (implant material, implant position, MAR condition, and kVp level) and their interactions on SD of the grey values, taking into account the existence of other factors. The power analysis considering the differences and variability observed among the groups reached 80%.

The analyses were performed using the SPSS v. 24.0 (IBM Corp., Armonk, NY) and GraphPad Prism v. 7.0 (GraphPad Software, La Jolla, CA) software, with a

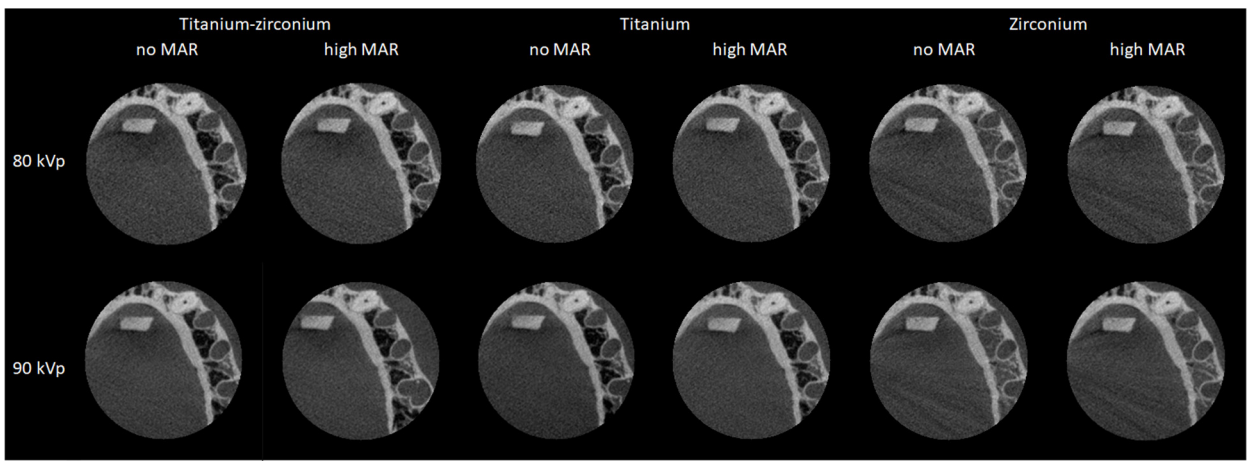

Figure 2 Representative CBCT axial images obtained with a 4 × 5 cm FOV according to the implant material, MAR condition, and kVp level. CBCT, cone-beam CT; FOV, field of view; MAR, metal artefact reduction.

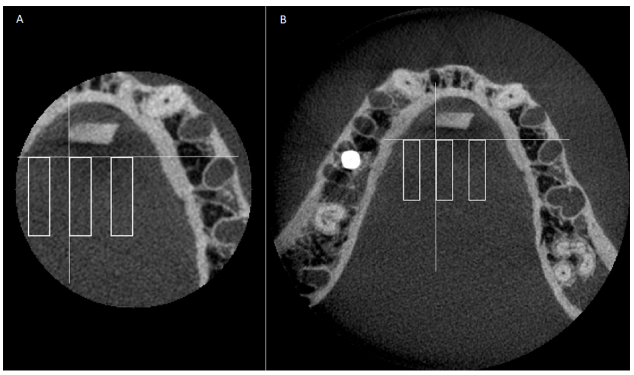

Figure 3 CBCT axial images indicating the three rectangular regions of interest: A. 4 × 5 cm FOV; B. 8 × 5 cm FOV. White lines are references for the placement of the middle ROI. ROI were established close to the implant, in the middle, and further from the implant, using a line tangent to the alveolar socket of second left premolar and a line perpendicular to the first and tangent to the ERBS block. From the intersection of those lines, the middle ROI was established. The close and further ROIs were drawn 3.6 mm from the middle ROI. . CBCT, cone-beam CT; FOV, field of view; ROI, region of interest.

significant level of 5% ($\alpha = 0.05$). The null hypothesis assumed that the factors investigated did not have any impact on SD of the grey values.

Results

Figure 4 shows mean values of SD of the grey values according to the factors studied. According to ANOVA, all factors (implant material, implant position, MAR condition, and kVp level) significantly influenced the values.

Regarding the effect of the implant material, in general, a zirconia implant produced significantly higher SD of the grey values (greater artefact expression) than a titanium–zirconium implant, which produced significantly higher SD of the grey values than a titanium implant ($p < 0.05$).

Regarding the influence of the implant position, in general, the artefacts were more pronounced with higher SD of the grey values in the 4 × 5 cm FOV (when the implant was in the exomass), than when the implant was inside the 8 × 5 cm FOV, as shown in Figure 4. Such a difference between FOV sizes is noticeable when comparing black and grey bars within the same kVp level and MAR condition. The black bars are higher than the grey ones, especially in the presence of titanium–zirconium and zirconia implants. Statistically significant greater SD of the grey values was observed for the 4 × 5 cm FOV in the following conditions: 80 kVp, titanium–zirconium implant, low and high MAR; 90 kVp, titanium–zirconium implant, high MAR; 80 kVp, titanium implant, low MAR; 80 and 90 kVp, zirconia implant, low and high MAR ($p < 0.05$). Such a significant difference was less frequent in the presence of the titanium implant, as it produced fewer artefacts and did not occur in control scans when there was no implant in the phantom ($p > 0.05$). Also, one can note that significant differences between FOV sizes only occurred when MAR was active (either at low or high levels), revealing that MAR was effective in decreasing SD of the grey values when the implant was inside the FOV, but not when the implant was in the exomass. This different behaviour of the action of the MAR increased the difference produced by the different positions of the implant.

MAR was effective in decreasing SD of the grey values only in some cases: 8 × 5 cm FOV, zirconia implant, 80 and 90 kVp ($p < 0.05$), which were the groups with the

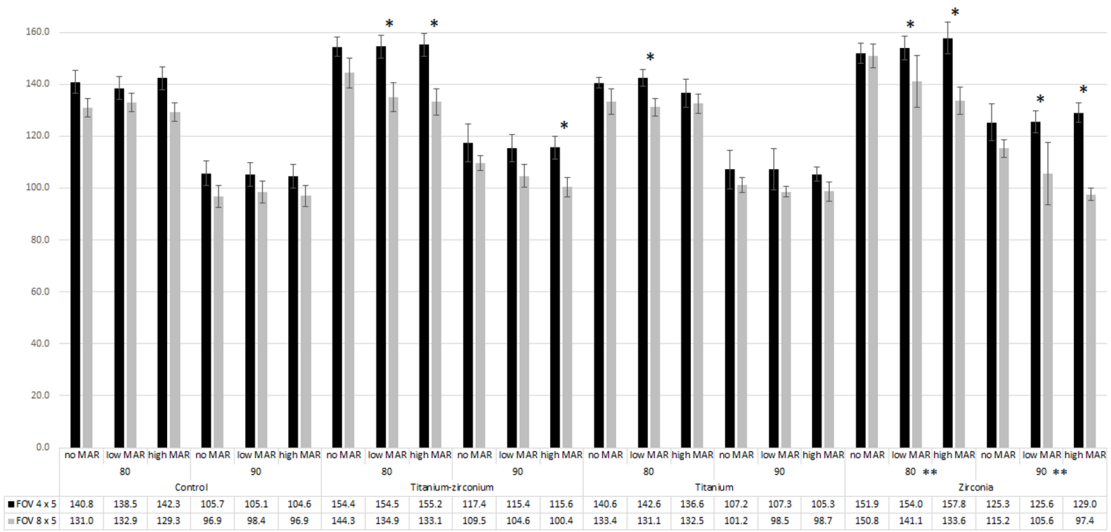

Figure 4 Mean of SD of the grey values according to the implant material, implant position, MAR condition, and kVp level. * indicates significant difference between SD of the grey values when the implant was in the exomass (4 × 5 cm FOV) and inside of the FOV (8 × 5 cm FOV). ** indicates significant difference only for 8 × 5 cm FOV between no MAR and low or high MAR. FOV, field of view; MAR, metal artefact reduction.

highest SD of the grey values when compared to the scans within the same conditions. In those cases, the high level of MAR was more effective. The effectiveness of MAR in 8 × 5 cm FOV in the presence of a zirconia implant is exemplified in Figure 4, as the height of grey bars (8 × 5 cm FOV) progressively decreases from "no MAR" to "high MAR" condition, whereas the black bars (4 × 5 cm FOV) remain stable.

Concerning the kVp level, 80 kVp produced images with higher SD of the grey values than 90 kVp, regardless of the other factors ($p < 0.05$).

Discussion

Among the factors affecting the radiation dose to the patient, the FOV size has been shown as one of the most important. Under identical exposure parameters, small-FOV sizes deliver less radiation and provide higher theoretical image quality.[5,16,17] Conversely, their use indirectly increases the exomass influence and manifestation of the truncation effect,[5,17,18,20] leading to inconsistencies in the reconstructed image.[1,5] Although large FOVs have been demonstrated to decrease CBCT voxel value variability,[5,16,20] their use cannot be justified only for the purpose of enhancing image quality because patients would be exposed to unnecessary high X-ray dose. Alternatively, priority should be given to the understanding of, and decreasing the artefacts from the exomass, when possible. There are only a few studies in the scientific literature investigating artefacts from high-density objects in the exomass,[5,19] and none of them have compared such artefacts with those produced by metal materials located inside of the FOV.

In general, dental implants led to greater artefact expression when located in the exomass than when inside the FOV, which is in agreement with a previous study evaluating three different CBCT units.[5] Oliveira et al[21] demonstrated a decrease in voxel value variability, thus artefact expression, when a uniform and thin layer of water was in the exomass, and hypothesised that the homogeneity of exomass should have behaved as an X-ray beam filter.

Materials presenting higher physical density and atomic number induce higher artefact expression while interacting with the X-ray beam.[5,22] Our findings with zirconia leading to greater artefact expression followed by the titanium–zirconium and titanium implants (atomic number for Zr = 40; Ti = 22; and *O* = 8) support this theory and also show that this tendency occurs even if the metal object is in the exomass.

The positive effect of increased kVp and MAR algorithm application in the reduction of artefacts is well-known.[10] Nevertheless, these parameters have been assessed in the literature mostly in the vicinity of the high-density objects. That is why we evaluated the effects of these parameters while implants were present both inside the FOV and in the exomass. This investigation is currently vital as numerous contemporary patients that undergo small-FOV CBCT scans have metal objects such as dental implants in the oral cavity. Therefore, finding the best parameter to reduce the artefact arising from materials both in the FOV or the exomass has clinical relevance.[5] Importantly, our findings showed that the increase of kVp had a positive effect by decreasing artefact expression even when the metal object was in the exomass.

Conversely, MAR algorithm had a positive effect on decreasing artefacts only when the metal object was inside the FOV, which is in accordance with a previous study.[19] A reduction of SD of the grey values exhibits a decrease in the artefact amount, which represents an actual function of MAR.[13] In our study, MAR acted when the artefact was more pronounced, *i.e.* with zirconia implant, similarly to the findings of previous studies.[2,13] In Queiroz et al.'s study,[13] MAR reduced the artefact arising from dental alloys, but not from gutta-percha. The authors referred to the fact that gutta-percha does not generate sufficient artefact to be reduced by MAR. In the same way, in our study, in scans with fewer artefacts, MAR effect was not observed, also supporting the theory how MAR works suggested by Queiroz et al.[13] The Planmeca ProMax CBCT unit allows for the selection of three levels of MAR: low, medium, or high. When one of these levels is selected, as explained in the Promax' user manual, the volume reconstruction ignores the voxels above and below a certain greyscale that have been marked by the threshold selection. Theoretically, by leaving the most heterogeneous areas out of the calculation, artefacts caused by high-density materials are decreased or removed.[19,23] However, the actual way MAR acts and its positive effects are still unknown. While some studies with high density objects inside the FOV showed that MAR did not decrease artefacts,[7,24] MAR enhanced image quality by reducing artefacts in other investigations.[2,10,25,26] In addition, this tool shows positive effect on the accuracy of approximal caries detection,[27] little or no influence on the diagnosis of peri-implant defects[23,28] and detection of fractured endodontic instruments,[29] and even negative impact on the diagnosis of root fracture.[15,30,31]

Because MAR is a post-processing tool, it does not alter the radiation dose delivered to the patient. Conversely, a linear relationship between kVp and the effective dose is not certain[32,33] and the FOV size has a clear influence on the effective dose.[32] As the present study did not perform dosimetry of the parameters studied, it is difficult to compare them in terms of radiation dose and to identify one of them based on the characteristics related to image quality evaluated here and on radioprotection principles. However, as FOV size is the main factor that affects radiation dose among those studies, we advocate that FOV size should be as small as possible based on the diagnostic task, but the professional must be aware of the ability of metal objects in the exomass to lead to greater artefact expression compared to when they are inside the FOV.

This study is one of very few that shed light on artefact generation from implant materials in the exomass and, to the best of the authors' knowledge, is the only study that compared artefact production when the metal material was inside the FOV *vs* the exomass. As an *in-vitro* study, we were able to have control of multiple variables affecting the results and to perform repeated CBCT scans of the same "patient". However, as a limitation, it is not possible to mimic the same implant-X-ray beam interaction of the clinical environment. Also, it is well-known that only experimental studies allow the investigators to analyse different exposure settings as it is not ethical to take images of patients just for research purposes. Additionally, in the clinical setting, radiographic exams acquired with a 4 × 5 cm FOV should have the area of interest centred in the FOV and not at the border of the exam as in the current study. However, this was necessary in order to have the same area to evaluate in both FOVs.

When translating our findings to a clinical situation, either titanium, titanium–zirconium, or zirconia implants produce artefacts, reducing the image quality even in sites far from the region of placement. Accordingly, artefacts from the exomass affect the assessment of other regions and could make diagnosis and treatment planning difficult. Clinicians should be aware that artefacts can have multiple presentations and arise from metal objects either in the FOV or in the exomass. Further studies and technological approaches are needed to overcome the exomass impact in CBCT.

Conclusion

The type of implant material as well as implant position influence artefact production. Implants located in the exomass lead to greater artefact expression compared to when they are inside the FOV. The MAR algorithm is efficient to decrease artefacts when they are more pronounced (with zirconia implant), but only when the implant is inside of the FOV and not in the exomass. Increasing kVp is also effective in decreasing artefact, regardless of whether its origin is inside the FOV or in the exomass.

Acknowledgement

This study was presented as a poster presentation in the 2019 Joint Conference of AAOMR & IADMFR in Philadelphia, PA.

Conflict of interest:

The authors declare that they have no conflict of interest.

Funding

This work was not financially supported by any organization or institution.

REFERENCES

1. Schulze R, Heil U, Gross D, Bruellmann DD, Dranischnikow E, Schwanecke U, et al. Artefacts in CBCT: a review. *Dentomaxillofac Radiol* 2011; **40**: 265–73. doi: https://doi.org/10.1259/dmfr/30642039
2. Freitas DQ, Fontenele RC, Nascimento EHL, Vasconcelos TV, Noujeim M. Influence of acquisition parameters on the magnitude of cone beam computed tomography artifacts. *Dentomaxillofac Radiol* 2018; **47**: 20180151. doi: https://doi.org/10.1259/dmfr.20180151
3. Fontenele RC, Nascimento EH, Vasconcelos TV, Noujeim M, Freitas DQ. Magnitude of cone beam CT image artifacts related to zirconium and titanium implants: impact on image quality. *Dentomaxillofac Radiol* 2018; **47**: 20180021. doi: https://doi.org/10.1259/dmfr.20180021
4. Vasconcelos TV, Bechara BB, McMahan CA, Freitas DQ, Noujeim M. Evaluation of artifacts generated by zirconium implants in cone-beam computed tomography images. *Oral Surg Oral Med Oral Pathol Oral Radiol* 2017; **123**: 265–72. doi: https://doi.org/10.1016/j.oooo.2016.10.021
5. Candemil AP, Salmon B, Freitas DQ, Ambrosano GM, Haiter-Neto F, Oliveira ML. Metallic materials in the exomass impair cone beam CT voxel values. *Dentomaxillofac Radiol* 2018; **47**: 20180011. doi: https://doi.org/10.1259/dmfr.20180011
6. Pauwels R, Jacobs R, Singer SR, Mupparapu M. CBCT-based bone quality assessment: are Hounsfield units applicable? *Dentomaxillofac Radiol* 2015; **44**: 20140238. doi: https://doi.org/10.1259/dmfr.20140238
7. Parsa A, Ibrahim N, Hassan B, van der Stelt P, Wismeijer D. Influence of object location in cone beam computed tomography (NewTom 5G and 3D Accuitomo 170) on gray value measurements at an implant site. *Oral Radiol* 2014; **30**: 153–9. doi: https://doi.org/10.1259/dmfr.20130329
8. Iikubo M, Osano T, Sano T, Katsumata A, Ariji E, Kobayashi K, et al. Root canal filling materials spread pattern mimicking root fractures in dental CBCT images. *Oral Surg Oral Med Oral Pathol Oral Radiol* 2015; **120**: 521–7. doi: https://doi.org/10.1016/j.oooo.2015.06.030
9. Chang E, Lam E, Shah P, Azarpazhooh A. Cone-Beam computed tomography for detecting vertical root fractures in Endodontically treated teeth: a systematic review. *J Endod* 2016; **42**: 177–85. doi: https://doi.org/10.1016/j.joen.2015.10.005
10. Helvacioglu-Yigit D, Demirturk Kocasarac H, Bechara B, Noujeim M. Evaluation and reduction of artifacts generated by 4 different Root-end filling materials by using multiple cone-beam computed tomography imaging settings. *J Endod* 2016; **42**: 307–14. doi: https://doi.org/10.1016/j.joen.2015.11.002
11. Ludlow JB, Timothy R, Walker C, Hunter R, Benavides E, Samuelson DB, et al. Effective dose of dental CBCT-a meta analysis of published data and additional data for nine CBCT units. *Dentomaxillofac Radiol* 2015; **44**: 20140197. doi: https://doi.org/10.1259/dmfr.20140197
12. Pinto MGO, Rabelo KA, Sousa Melo SL, Campos PSF, Oliveira LSAF, Bento PM, et al. Influence of exposure parameters on the detection of simulated root fractures in the presence of various intracanal materials. *Int Endod J* 2017; **50**: 586–94. doi: https://doi.org/10.1111/iej.12655
13. Queiroz PM, Oliveira ML, Groppo FC, Haiter-Neto F, Freitas DQ. Evaluation of metal artefact reduction in cone-beam

computed tomography images of different dental materials. *Clin Oral Investig* 2018; **22**: 419–23. doi: https://doi.org/10.1007/s00784-017-2128-9
14. Queiroz PM, Santaella GM, da Paz TDJ, Freitas DQ. Evaluation of a metal artefact reduction tool on different positions of a metal object in the FOV. *Dentomaxillofac Radiol* 2017; **46**: 20160366. doi: https://doi.org/10.1259/dmfr.20160366
15. Bechara B, Alex McMahan C, Moore WS, Noujeim M, Teixeira FB, Geha H. Cone beam CT scans with and without artefact reduction in root fracture detection of endodontically treated teeth. *Dentomaxillofac Radiol* 2013; **42**: 20120245. doi: https://doi.org/10.1259/dmfr.20120245
16. Pauwels R, Jacobs R, Bogaerts R, Bosmans H, Panmekiate S. Reduction of scatter-induced image noise in cone beam computed tomography: effect of field of view size and position. *Oral Surg Oral Med Oral Pathol Oral Radiol* 2016; **121**: 188–95. doi: https://doi.org/10.1016/j.oooo.2015.10.017
17. Farman AG. Field of view. *Oral Surg Oral Med Oral Pathol Oral Radiol Endod* 2009; **108**: 477–8. doi: https://doi.org/10.1016/j.tripleo.2009.04.001
18. Meilinger M, Schmidgunst C, Schütz O, Lang EW. Metal artifact reduction in cone beam computed tomography using forward projected reconstruction information. *Z Med Phys* 2011; **21**: 174–82. doi: https://doi.org/10.1016/j.zemedi.2011.03.002
19. Candemil AP, Salmon B, Freitas DQ, Ambrosano GMB, Haiter-Neto F, Oliveira ML. Are metal artefact reduction algorithms effective to correct cone beam CT artefacts arising from the exomass? *Dentomaxillofac Radiol* 2019; **48**: 20180290. doi: https://doi.org/10.1259/dmfr.20180290
20. Katsumata A, Hirukawa A, Okumura S, Naitoh M, Fujishita M, Ariji E, et al. Relationship between density variability and imaging volume size in cone-beam computerized tomographic scanning of the maxillofacial region: an in vitro study. *Oral Surg Oral Med Oral Pathol Oral Radiol Endod* 2009; **107**: 420–5. doi: https://doi.org/10.1016/j.tripleo.2008.05.049
21. Oliveira ML, Freitas DQ, Ambrosano GMB, Haiter-Neto F. Influence of exposure factors on the variability of CBCT voxel values: a phantom study. *Dentomaxillofac Radiol* 2014; **43**: 20140128. doi: https://doi.org/10.1259/dmfr.20140128
22. Kuusisto N, Vallittu PK, Lassila LVJ, Huumonen S. Evaluation of intensity of artefacts in CBCT by radio-opacity of composite simulation models of implants in vitro. *Dentomaxillofac Radiol* 2015; **44**: 20140157. doi: https://doi.org/10.1259/dmfr.20140157
23. de-Azevedo-Vaz SL, Peyneau PD, Ramirez-Sotelo LR, Vasconcelos KdeF, Campos PSF, Haiter-Neto F. Efficacy of a cone beam computed tomography metal artifact reduction algorithm for the detection of peri-implant fenestrations and dehiscences. *Oral Surg Oral Med Oral Pathol Oral Radiol* 2016; **121**: 550–6. doi: https://doi.org/10.1016/j.oooo.2016.01.013
24. Vasconcelos KF, Nicolielo LFP, Nascimento MC, Haiter-Neto F, Bóscolo FN, Van Dessel J, et al. Artefact expression associated with several cone-beam computed tomographic machines when imaging root filled teeth. *Int Endod J* 2015; **48**: 994–1000. doi: https://doi.org/10.1111/iej.12395
25. Demirturk Kocasarac H, Helvacioglu Yigit D, Bechara B, Sinanoglu A, Noujeim M. Contrast-to-noise ratio with different settings in a CBCT machine in presence of different root-end filling materials: an in vitro study. *Dentomaxillofac Radiol* 2016; **45**: 20160012. doi: https://doi.org/10.1259/dmfr.20160012
26. Fontenele RC, Nascimento EHL, Santaella GM, Freitas DQ. Does the metal artifact reduction algorithm activation mode influence the magnitude of artifacts in CBCT images? *Imaging Sci Dent* 2020; **50**: 23–30. doi: https://doi.org/10.5624/isd.2020.50.1.23
27. Cebe F, Aktan AM, Ozsevik AS, Ciftci ME, Surmelioglu HD. The effects of different restorative materials on the detection of approximal caries in cone-beam computed tomography scans with and without metal artifact reduction mode. *Oral Surg Oral Med Oral Pathol Oral Radiol* 2017; **123**: 392–400. doi: https://doi.org/10.1016/j.oooo.2016.11.008
28. Sheikhi M, Behfarnia P, Mostajabi M, Nasri N. The efficacy of metal artifact reduction (MAR) algorithm in cone-beam computed tomography on the diagnostic accuracy of fenestration and dehiscence around dental implants. *J Periodontol* 2020; **91**: 209–14. doi: https://doi.org/10.1002/JPER.18-0433
29. Costa ED, Brasil DM, Queiroz PM, Verner FS, Junqueira RB, Freitas DQ. Use of the metal artefact reduction tool in the identification of fractured endodontic instruments in cone-beam computed tomography. *Int Endod J* 2020; **53**: 506–12. doi: https://doi.org/10.1111/iej.13242
30. Bezerra ISQ, Neves FS, Vasconcelos TV, Ambrosano GMB, Freitas DQ. Influence of the artefact reduction algorithm of Picasso trio CBCT system on the diagnosis of vertical root fractures in teeth with metal posts. *Dentomaxillofac Radiol* 2015; **44**: 20140428. doi: https://doi.org/10.1259/dmfr.20140428
31. Oliveira MR, Sousa TO, Caetano AF, de Paiva RR, Valladares-Neto J, Yamamoto-Silva FP, et al. Influence of CBCT metal artifact reduction on vertical radicular fracture detection. *Imaging Sci Dent* 2021; **51**: 55–62. doi: https://doi.org/10.5624/isd.20200191
32. Al-Okshi A, Horner K, Rohlin M. A meta-review using the ROBIS tool of effective doses in dental and maxillofacial cone beam CT. *Br J Radiol* 2021; **14**: 20210042.
33. Van Acker JWG, Pauwels NS, Cauwels RGEC, Rajasekharan S. Outcomes of different radioprotective precautions in children undergoing dental radiography: a systematic review. *Eur Arch Paediatr Dent* 2020; **21**: 463–508. doi: https://doi.org/10.1007/s40368-020-00544-8